

International Conference on Space Optics—ICSO 2018

Chania, Greece

9–12 October 2018

Edited by Zoran Sodnik, Nikos Karafolas, and Bruno Cugny



Alignment procedure for the Gregorian telescope of the Metis coronagraph for the Solar Orbiter ESA mission

Vania Da Deppo

Sergio Mottini

Giampiero Naletto

Fabio Frassetto

et al.



icso proceedings



Alignment procedure for the Gregorian telescope of the Metis coronagraph for the Solar Orbiter ESA mission

Vania Da Deppo^{*a,b}, Sergio Mottini^c, Giampiero Naletto^{d,a,b,e}, Fabio Frassetto^a, Paola Zuppella^a, Mewael G. Sertsu^f, Marco Romoli^g, Silvano Fineschi^h, Ester Antonucci^h, Gianalfredo Nicolini^h, Piergiorgio Nicolosiⁱ, Daniele Spadaro^j, Vincenzo Andretta^k, Marco Castronuovo^l, Marta Casti^h, Gerardo Capobianco^h, Giuseppe Massone^h, Roberto Susino^h, Federico Landini^m, Maurizio Pancrazzi^g, Chiara Casini^g, Luca Teriacaⁿ, Michela Uslenghi^o

^aCNR-Istituto di Fotonica e Nanotecnologie, Padova, Via Trasea 7, 35131 Padova, Italy; ^bINAF-Osservatorio Astronomico di Padova, Vicolo dell'Osservatorio 5, 35122 Padova, Italy; ^cThales Alenia Space Italia, Strada Antica di Collegno 253, 10146 Torino, Italy; ^dDipartimento di Fisica e Astronomia "Galileo Galilei" - Università degli Studi di Padova, Via Marzolo 8, 35131 Padova, Italy; ^eCISAS Centro Interdipartimentale Studi e Attività Spaziali "G. Colombo", Via Venezia 15, 35131 Padova, Italy; ^fDepartment of Nanometer Optics and Technology, Helmholtz-Zentrum Berlin, Albert-Einstein str. 15, 12489 Berlin, Germany; ^gDipartimento di Fisica ed Astronomia - Università degli Studi di Firenze, Via G. Sansone 1, 50019 Sesto Fiorentino (Fi), Italy; ^hINAF - Osservatorio Astrofisico di Torino, Strada Osservatorio 20, 10025 Pino Torinese (To), Italy; ⁱDipartimento di Ingegneria dell'Informazione, Università di Padova, Via Gradenigo 6/B, 35131 Padova; ^jINAF-Osservatorio Astrofisico di Catania, Via S. Sofia 78, 95123 Catania, Italy; ^kINAF-Osservatorio Astronomico di Capodimonte, Salita Moiariello 16, 80131 Napoli, Italy; ^lASI, Via del Politecnico, 00133 Roma, Italy; ^mINAF-Osservatorio Astrofisico di Arcetri, Largo E. Fermi 5, 50125 Firenze, Italy; ⁿMax Planck Institute for Solar System Research, Justus-von-Liebig-Weg 3, 37077 Göttingen, Germany; ^oINAF-IASF, Via E. Bassani, 20133 Milano, Italy

ABSTRACT

Metis is a solar coronagraph mounted on-board the Solar Orbiter ESA spacecraft. Solar Orbiter is scheduled for launch in February 2020 and it is dedicated to study the solar and heliospheric physics from a privileged close and inclined orbit around the Sun. Perihelion passages with a minimum distance of 0.28 AU are foreseen.

Metis features two channels to image the solar corona in two different spectral bands: in the HI Lyman α at 121.6 nm, and in the polarized visible light band (580 – 640 nm). Metis is a solar coronagraph adopting an "inverted occulted" configuration. The inverted external occulter (IEO) is a circular aperture followed by a spherical mirror which back rejects the disk light. The reflected disk light exits the instrument through the IEO aperture itself, while the passing coronal light is collected by the Metis telescope. Common to both channels, the Gregorian on-axis telescope is centrally occulted and both the primary and the secondary mirror have annular shape.

Classic alignment methods adopted for on-axis telescope cannot be used, since the on-axis field is not available. A novel and ad hoc alignment set-up has been developed for the telescope alignment.

An auxiliary visible optical ground support equipment source has been conceived for the telescope alignment. It is made up by four collimated beams inclined and dimensioned to illuminate different sections of the annular primary mirror without being vignetted by other optical or mechanical elements of the instrument.

Keywords: alignment procedures, coronagraph, Gregorian telescope, auxiliary OGSE source

*vania.dadeppo@ifn.cnr.it; phone +39-049 9815639

1. INTRODUCTION

Solar Orbiter (SO) is a mission dedicated to study solar and heliospheric physics [1]. It was selected as the first medium-class mission of ESA's Cosmic Vision 2015-2025 Programme. With a combination of in-situ and remote sensing instruments, SO is conceived for the circumsolar region exploration with the purpose of giving an answer to the scientific questions on how the heliosphere is generated and controlled by the Sun.

Scheduled for launch in February 2020, the mission will provide close-up, high-latitude observations of the Sun. SO will have a highly elliptic orbit – between 0.9 AU at aphelion and 0.28 AU at perihelion. It will reach its operational orbit three-and-a-half years after launch by using gravity assist maneuvers (GAMs) at Earth and Venus. Subsequent GAMs at Venus will increase its inclination to the solar equator over time, reaching up to 25° at the end of the nominal mission (approximately 7 years after launch) and up to 34° in the extended mission phase.

Metis is one of the remote sensing instruments mounted on-board the SO spacecraft. The Metis coronagraph has been conceived to acquire both visible and UV images of the solar corona. It has two channels: one to study the UV HI Lyman α at 121.6 nm, and the other for the polarized visible light band (580 – 640 nm).

Metis adopts a configuration called ‘inverted externally occulted’ that is able to prevent the solar disk light to enter the telescope; this light is back reflected outside by a mirror (M0). The passing coronal light is collected by the Metis telescope. Common to both channels, the Gregorian on-axis telescope is centrally occulted and both the primary and the secondary mirrors have annular shape. Moreover, the on-axis field is not available since it is anyway completely blocked by the M0 mirror. A novel and ad hoc alignment set-up has been developed for the telescope alignment [2] [3].

In particular, an auxiliary visible optical ground support equipment source has been conceived to align the primary and secondary mirror. It is made up by four collimated beams inclined and dimensioned to illuminate different sections of the annular field of view without being vignetted by the optical or mechanical elements of the instrument.

The integration and alignment, performed by the Thales Alenia Space integration team, and the on-ground calibrations of Metis have been accomplished in an ISO5 environment at the Optical Payload System (OPSys), a laboratory of the INAF Astrophysical Observatory of Torino hosted by ALTEC S.p.A. in Torino (Italy).

In this paper, after a description of the Metis optical design and performance, the telescope alignment philosophy, the adopted set-up, the parameters used for the analysis and the obtained results for the Metis proto flight model alignment are described.

2. METIS OPTICAL DESIGN AND PERFORMANCE

2.1 Metis optical design

The Metis instrument is conceived to image the solar corona from a near-Sun orbit in two different spectral bands: the UV narrow band HI Lyman- α at 121.6 nm, and the polarized broad-band visible light (580 – 640 nm). The instrument is designed to image the structure and dynamics of the full corona in the range from 1.6 to 3.1 solar radii (R_s), at minimum perihelion distance (0.28 AU), and from 2.8 R_s to 5.4 R_s , at 0.5 AU. The annular Field of View (FoV) covered by the instrument is between 1.6° and 2.9° , and the attained spatial resolution is 20 arcsec.

The “inverted external occulted” configuration (see Figure 1) [4][5] allows to reduce the thermal loads inside the instrument. The inverted external occulter (IEO), a small aperture on the spacecraft thermal shield, also acts as the entrance pupil of the instrument. The solar disk light passing through the IEO is back-reflected by a spherical heat-rejection mirror (M0) and focused on the IEO itself. The coronal light, on the other hand, is collected by an on-axis Gregorian telescope.

The primary mirror (M1) focalizes the gathered coronal light in its focal plane, where a field stop (FS) is placed and limits the outer FOV of the coronagraph. Then the secondary mirror (M2) focalizes the light again; part of the light passes through the interference filter (IF) and then is collected by UV detector; the other part is reflected by the IF and is directed to the polarimeter module.

Stray light minimization is a mandatory goal in any coronagraph and the worst offenders are the surfaces hit by the direct solar disk light, IEO and M0. The internal occulter (IO) and the Lyot stop (LS) are, respectively, conjugated with the IEO and M0 via the primary mirror M1. IO blocks the solar disk light diffracted by the IEO edge, while LS blocks the light diffracted by the M0 edge [6][7].

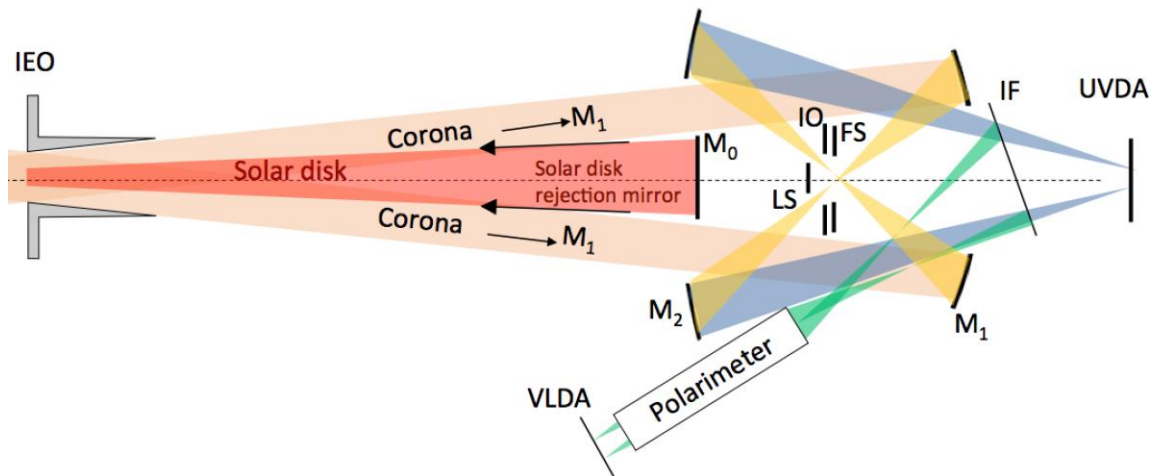


Figure 1. Metis layout. Schematic view of the inverted-occulted coronagraph optical layout (not to scale) [6].

Metis consists of a single optical head which incorporates 2 different channels: an UV imaging channel and a polarimetric visible light (VL) channel. The telescope optics (M1 and M2) and the stop system (IEO, M0, FS, IO and LS) are common to both channels, while the VL channel has a dedicated relay optics and a polarizing group. Each channel has its own detector respectively called UVDA and VLDA.

The Metis instrument optical specifications are summarized in Table 1.

Table 1 Summary of Metis instrument optical characteristics.

<u>Metis instrument optical specifications</u>	
FoV	1.6°-2.9° 1.7-3.1 R _s @ 0.28 AU – 3.0-5.4 R _s @ 0.5 AU
Telescope type	Externally occulted on-axis Gregorian
Effective focal length	VL: 200 mm UV: 300 mm
Wavelength range	VL: 580-640 nm UV: 121.6 ± 10 nm
Spatial resolution	VL: < 20 arcsec @ > 2° < 40 arcsec @ < 2° UV: < 20 arcsec
Average Straylight (B _{cor} /B _{sun})	VL < 10 ⁻⁹ UV < 10 ⁻⁷
Detectors	VL: 2048x2048 10 μm pixel size UV: 1024x1024 30 μm pixel size

2.2 UV and Visible-light imaging paths

The coronal light collected by the Metis Gregorian on-axis telescope is divided in two different paths:

- narrow band ultraviolet HI Lyman α (121.6 nm) path;
- polarized visible-light (580-640 nm) path.

The two different UV and VL paths are separated through an UV interference filter (IF), inserted in the converging beam exiting M2, and inclined at 12° with respect to the optical axis of the telescope. The UV narrow bandpass interference filter acts as VL-UV dichroic beam splitter by selecting the 121.6 nm UV band in transmission and reflecting the VL.

The mirrors are coated with Al+MgF₂ with high reflectivity in the VL band and optimized to have an enhanced reflectivity at 121.6 nm [8] [9].

Inside the polarimetric path a broad band filter selects the VL bandpass (580-640 nm). The VL polarimeter sub-channel includes a polarization group (PG), comprising a modulation package (PMP) with a liquid crystal variable retarder (LCVR) together with a fixed quarter-wave retarder and a linear polarizer in “Senarmont” configuration [10][11]. The PG is placed in-between a relay optics system that collimates, through the PG, the linearly polarized VL from the K-corona and refocuses it on the VL detector.

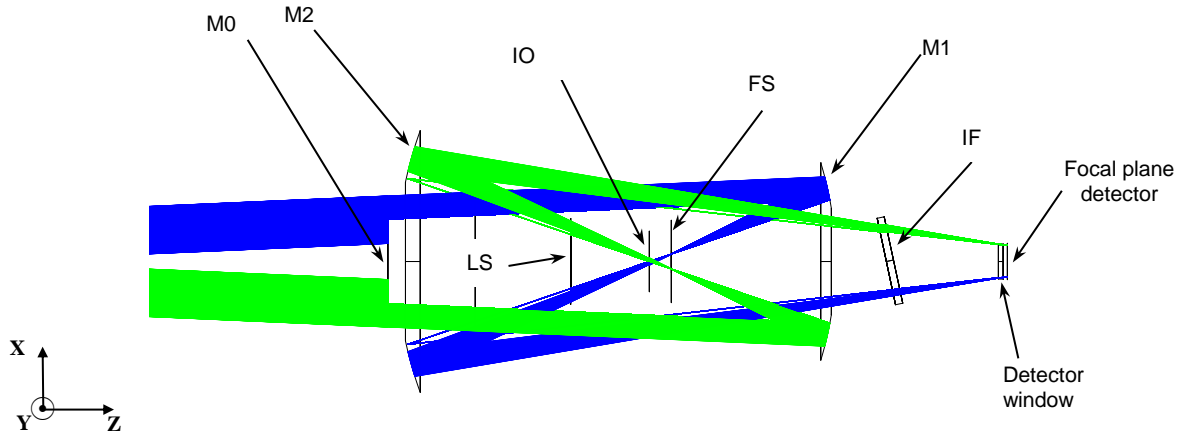


Figure 2. Metis telescope layout. For clarity, only the raytraces for two angular field positions ($\pm 2.5^\circ$) are depicted.

The optical characteristics of the 300-mm focal length telescope system common to both paths are reported in Table 2.

Table 2 Summary of Metis Gregorian telescope characteristics.

Parameter	Value
Entrance pupil diameter	40 mm
M1 curvature radius	272 mm
M2 curvature radius	312.4 mm
M2 magnification	2.2
M1-M2 distance	363 mm
Back focal length	500 mm

In Figure 2, to allow to follow the optical layout inside the telescope, the path of two incoming beams at field angles $\pm 2.5^\circ$ is depicted for the UV channel. Note that the incoming light is highly vignetted by M0 and partly vignetted by the IO and LS. Over the nominal FoV of the telescope the fraction of unvignetted rays is always less than 50%.

2.3 Estimated UV and Visible-light imaging path optical performance

The estimated optical performance of the UV and VL telescope paths, including the calculation of the diffraction effect, is shown in Figure 3. In Figure 3(b) the calculated RMS spot radius at the telescope focus is compared with an equivalent pixel size for both the UV and VL paths. For the UV the equivalent size is simply half of the UV detector pixel size, while for the VL channel it is 7.5 μm taking into account the effects of the polarimetric module. In fact it has a magnification of 0.67; thus the 10 μm pixel placed in the VL channel focal plane corresponds to a 15 μm pixel in the telescope focal plane.

The VL path aberrations are rather limited as it can be seen in Figure 4; the geometrical VL spot diagrams are depicted only for a radial slice in the FoV, since the VL channel design is perfectly radial symmetric. This is not the case for the UV path. The IF is a thick 6 mm tilted plate placed in a converging beam, thus some aberrations (mainly astigmatism and coma) are introduced by the filter [12]. To mitigate these aberrations, the filter surfaces are not parallel but tilted by about 0.15° .

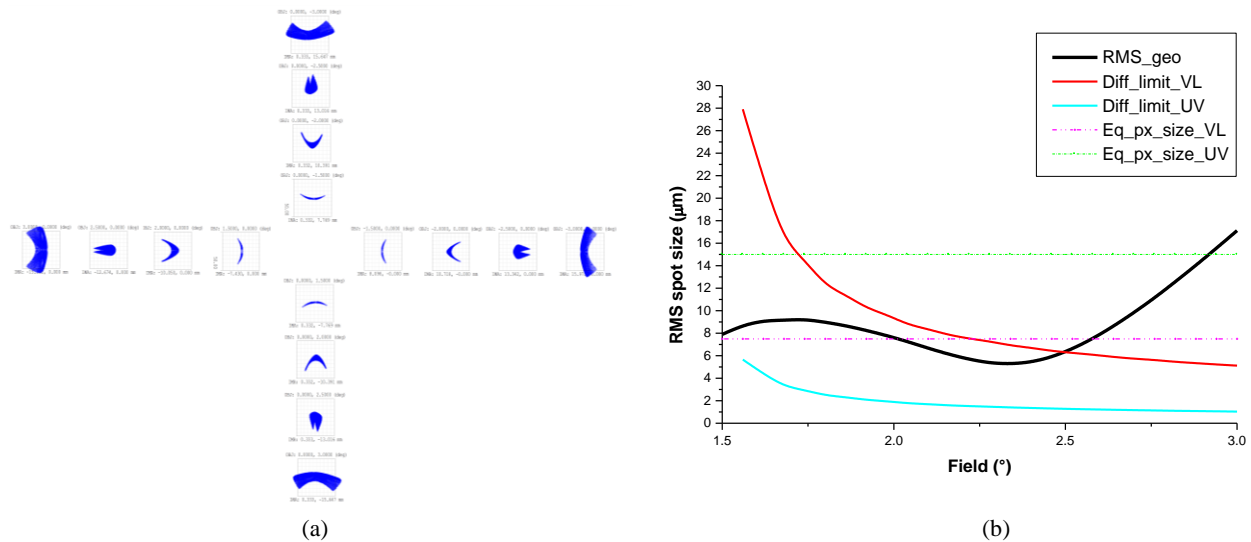


Figure 3. Metis telescope performance. (a) Geometric spot diagrams versus FoV (the square boxes have 50 micron size). (b) Mean geometrical RMS spot radius versus FoV compared with the diffraction limited RMS spot size and with the detector equivalent pixel size, both for the UV and VL paths.

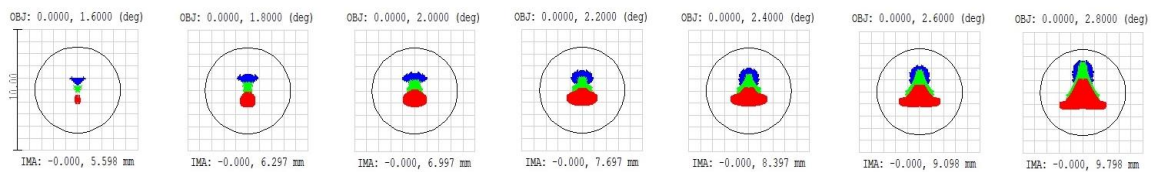


Figure 4. Geometrical spot diagrams for the VL channel. The square boxes have 10 micron size. In red the 610 nm wavelength, and in blue and green respectively the 580 and 640 nm ones, i.e. the central and the edge wavelengths in the considered range (580-640 nm).

3. TELESCOPE ALIGNMENT

3.1 Alignment philosophy

The alignment of the Metis optical components has been realized mainly metrologically, that is through the use of mechanical references and optical auxiliary instruments such as sighting telescope and theodolite. Only in a few cases it has been possible to drive the alignment by evaluating the optical performance on the focal plane.

Due to the opto-mechanical concept of the instrument, completely enclosed in its mechanical structure, with absolutely no accessibility from outside and with limited accessibility during integration, the alignment was strictly interlaced with the integration sequence. Each successive integration step was authorized only after the successful achievement of the previous alignments. The alignment and integration procedure has been determined on the basis of the tolerance analysis performed during the instrument design phase [13][14].

Both M1 and M2 are equipped with a reference surface (ARS) orthogonal to the optical axis and a centering target (CT). The first element to be provisionally integrated in the Metis structure is M2; its ARS and CT allow to define the direction and the position of the Metis optical axis. Then M1 is provisionally integrated in the structure too, and its ARS and CT are used to adjust its position and rotation for aligning it with M2 [2]. At this point a plane parallel plate (PPP) is located in front of Metis and aligned perpendicular to the Metis optical axis and a co-aligned sighting telescope is installed on the opposite side, so creating an external reference for the instrument optical axis and line of sight. This last step is necessary because, to integrate the internal elements M0 and IO, it is necessary to remove the two mirrors, so losing the optical axis reference; moreover, their insertion inhibits the possibility to look along the system optical axis.

Once the external Metis axis reference has been defined, both mirrors are removed and the integration and alignment of the IO/FS assembly is realized first, followed by the M0/LS one (see Figure 5 to locate the different parts inside Metis envelope). Then M2 is integrated and checked via the sighting telescope and M1 is mechanically integrated again (note that

this second integration of the two mirrors strongly relies on the repeatability of the mirror mechanical repositioning). The distance between M1 (adjustable) and M2 (fixed) is corrected with the use of an auxiliary visible detector mounted in the nominal focal plane of the telescope. The nominal focal plane has been determined via raytracing. It has to be taken into account that the UV channel telescope focal position is slightly different from the telescope one, because the IF (6 mm thick MgF₂) and the optical window mounted in front of the UVDA flight detector (4 mm thick MgF₂) introduce a focus shift of about 3.8 mm.

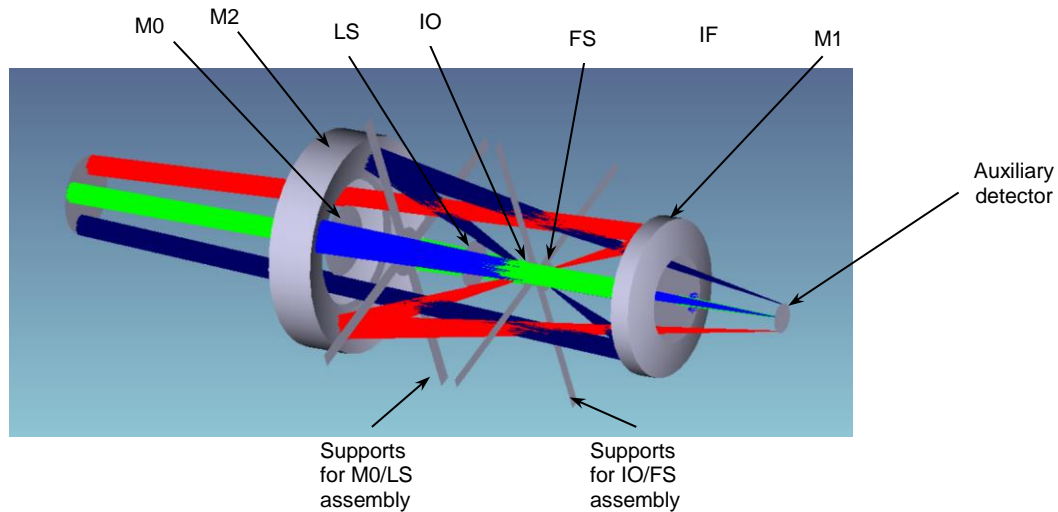


Figure 5. Ray-trace of the four-beam source used for the alignment of the Metis telescope. All the internal elements and their mounts are also depicted.

Even if used as compensator, a good pre-alignment of M1 was important to ensure the final result. The compensation of decentering errors with tilt adjustments to suppress coma, would have been efficient only for small errors. For this reason, an integration accuracy of 20" in tilt and 80 μm in centering has been requested.

3.2 Auxiliary alignment source

The alignment of the telescope, i.e. of M1 and M2, with the expected accuracy requires a purely optical feedback based on the imaging performance of the system. The performance is evaluated through 3 different parameters:

- the control of the image plate scale, in order to restore the correct focal length and magnification;
- the control of the image position, in order to minimize extra-axial aberrations due to centering and tilt errors;
- the control of the spot size, in order to maximize the Ensquared Energy.

The first two geometrical parameters are nominally sufficient to correctly align the UV channel; the spot size is instead used for the VL channel, where the plate scale could be slightly different from the nominal one (max 2%) due to the adjustment of M1 position.

An auxiliary alignment source has been designed (see Figure 6) to align the Metis telescope and obtain the visible channel optical performance at once. To be able to balance the performance across the field of view, the source is conceived to test Metis simultaneously in 4 different symmetric angular directions around the reference axis. Starting from a fiber pigtailed laser source at 635 nm, the device delivers four 20-mm diameter (at 1/e²) collimated beams as it is shown in Figure 6a. The size of the beams has been chosen as the result of the trade-off between vignetting and diffraction to obtain the best possible optical accuracy.

The four Metis angular fields sampled by the source are: (0°, 2.5°), (0°, -2.5°), (2.5°, 0°), (-2.5°, 0°). The reference (0°, 0°) axis shall be aligned with the Metis reference axis. The admissible error is 0.1°. The four beams diameter, position and direction, have been designed to hit M1 without being vignettted by the preceding elements. The four beams are generated from a single beam entering an assembly of beam-splitter cubes cemented together. A picture of the assembled source is shown in Figure 6b.

The source assembly provides some references for its alignment in the setup. In particular, there is a reference surface, located in correspondence of the source axis, which is normal to the reference direction ($0^\circ, 0^\circ$) and hosts also a reference for centering. The reference surface can be observed in autocollimation for tip/tilt adjustment and the centering target seen by a sighting telescope. To be able to reach a successful alignment, the directions and the position knowledge accuracy with respect to the reference surfaces should be better than 0.01° and ± 0.5 mm, respectively. While centering is not demanding, the tilt accuracy requires the use of a dedicated tilting platform. In principle roll can also be adjusted, but in practice, the rotation about the reference axis has not been considered of interest since the image analysis software provides size and symmetry of the image regardless of its rotation. The distance of the source from the telescope is not critical, its tolerance is of the order of millimeters of tolerance).

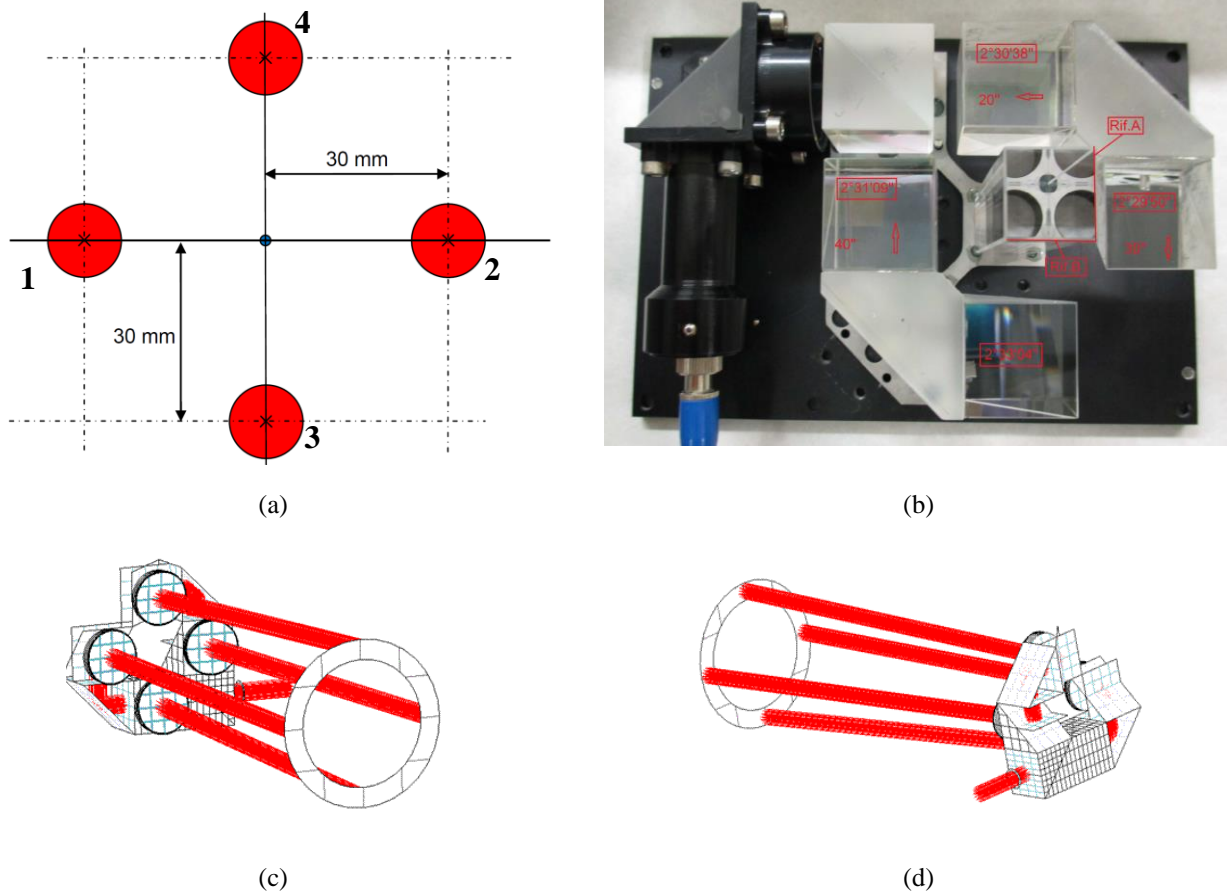


Figure 6. The four-beam auxiliary alignment source. (a) Layout at the exit port (footprint of the sources not to scale). (b) A picture. (c) and (d) front and rear views of the ray tracing in CODEV through the source.

By means of this auxiliary source, the position of the Metis UV detector is achieved by measuring the geometrical characteristics of the image (scale and position) provided by the telescope (M1+M2) on the auxiliary detector. The final alignment of the VL channel, instead, is reached through the optimization of spot size (ensquared energy) on the UVDA flight detector, since the VL plate scale could have been slightly affected (max 2%) by the previous M1 longitudinal adjustment. The alignment is performed at room temperature.

To provide a feedback in terms of plate scale (image size) and image position (with respect to the reference axis) of the 4-beam source, the camera selection has been driven by the capability of providing a wide enough field of view to collect the four beams, and a pixel size to adequately estimate the spots positions, i.e. determine the centroid with sub-pixel accuracy.

The selected camera model is the FLI ProLine PL50100, whose sensor specifications are summarized in Table 3.

Table 3 Auxiliary camera characteristics.

Parameter	Value
Sensor	Truesense KAF-50100
Pixels	8176 x 6132 (50 Mpixels)
Pixel size	6 μm
Sensor size	49 mm x 36.7 mm
Anti-blooming	800x

The software for acquiring and compute the figures of merit has been developed by the TASI optical team in Labview environment.

3.3 Alignment simulation and results

The auxiliary alignment source has been characterized by the producer and the outcoming direction of each beam has been measured. Using these measurements, i.e. the angular direction of the four beams, a raytracing has been done to determine the spot position and dimensions on the auxiliary detector. The expected spot diagrams are reported in Figure 7A.

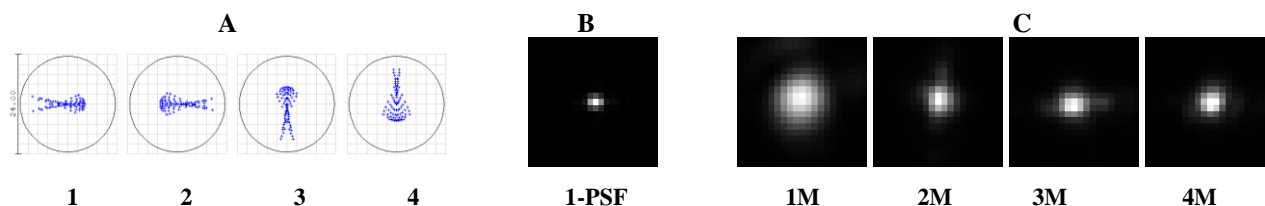


Figure 7. Comparison among the ray-traced spot diagram (A), the expected (B) and measured (C) spots on the auxiliary detector. In (A) the theoretical spot diagrams 1, 2, 3, 4 are depicted. The scale is 24 microns, corresponding to 4 x4 pixels of the auxiliary detector; the circle represents the Airy disk. In (B) the simulated theoretical point-source PSF on the detector. In (C) real measured spot at the considered best telescope alignment.

The four beams have been numbered 1, 2, 3, 4 (see Figure 6), which on the detector corresponds to right and left (1,2) and low and high (3,4); the spots are almost located along the x and y axis on the detector. The expected Airy diameter is 23 μm , corresponding to approximately 4x4 pixel of the auxiliary detector. A simulation of the expected theoretical image on the detector is reported in Figure 7B. The box is 20x20 pixels, each pixel has 6 μm dimension as the pixels of the auxiliary detector.

The expected distance between the four points has been derived. The distance between 1 and 2 is expected to be 26.07 mm and the one between 3 and 4 26.31 mm.

In Figure 7C the spot obtained for the final alignment are given. The measured distances between the spots (1,2) and (3,4), 26.03 mm and 26.30 mm respectively, assure that the scale is correctly set to the theoretical value. The spots dimension is however larger than expected, being the FWHM of the order of 3 to 6 px, with respect to the foreseen 1.5-2.5 px. Diffusion and cross talk between adjacent pixels can justify a slightly larger dimension with respect to the expected one, but are not considered fully responsible for the whole enlargement. This has been justified also by considering a not-perfect collimation of the auxiliary source beams.

The correct verification of the image symmetry, with respect to the Metis reference axis, has requested a preliminary alignment phase in which the projection of the reference axis on the detector, i.e. a reference pixel, has been identified. The only way to identify the reference pixel was to project the sighting telescope beam, which is the materialization of the reference axis generated by M2. As explained in Section 3.1, the external reference axis has been defined in the very initial phase of the alignment, when all the internal elements were not yet present.

The focus adjustment on the visible channel has been based on image quality rather than on its geometry (plate scale) [2], in fact the distance between the telescope focus and the polarimeter module, after the M1 and M2 alignment, was not any longer the nominal one. Once the VLDA is integrated in its fixed position and given the actual conjugates distance, the magnification produced by the polarimeter module is not expected to be the nominal one and it does not correspond to the expected image quality. The resulting plate scale matches the design with an error of about 2%, fully acceptable, as

predicted by the Monte Carlo simulation of the full procedure. For the alignment of the visible channel, being able to operate in air, the VLDA flight model has been used.

4. CONCLUSIONS

The experimental set-up adopted for the alignment of the Gregorian telescope of the Metis instrument for the Solar Orbiter mission has been described. The telescope is the core part of the Metis coronagraph and it is common to both the channels (UV and VL) of the instrument.

Being the system centrally occulted, an ad hoc auxiliary light source has been designed to off-axis illuminate the system without being vignetted by optical elements and stops present in the system. This guarantees the alignment of the primary and secondary mirror to the necessary level of accuracy.

The auxiliary light source provides four 20-mm in diameter collimated beams inclined at 2.5° with respect to the axis of the telescope. The generated spots, acquired on an auxiliary camera, have guided the alignment process. Following the tolerance analysis done for the instrument, the scale on the auxiliary detector has been used as a target parameter for the correct alignment of the UV channel. The adjustment of M1 position perturbs the magnification of the visible channel, mechanically fixed. Hence, the visible detector adjustment has given priority to the optimization of the Ensquared Energy, tolerating a maximum change in the plate scale of 2%, as predicted by Monte Carlo simulations.

As a lesson learned, it would be helpful to know not only the inclination of the auxiliary source with respect to the optical axis, but also the degree of collimation of the beams. The possibility to check also the optical quality through a through focus allows to have a better confidence on the obtained alignment.

ACKNOWLEDGMENTS

This work has been supported by the Italian Space Agency (ASI) under a contract with the National Institute of Astrophysics (INAF), 'Accordo Addendum I/013/12/1', and with the co-financing of INAF, and under the contract with the industrial partners: ASI-ATI N. 2013-057-I.0.

The design, development, implementation and test of Metis have been performed by an industrial consortium constituted by OHB Italia (acting as Prime Contractor towards ASI with the specific responsibility of system engineering, the optical subsystems, the electronics and the basic software) and Thales Alenia Space Italia (Co-Prime Contractor with the specific responsibility of the telescope configuration and thermo-mechanical subsystems, the application software and the instrument AIT). ALTEC Company, as sub-contractor, provided logistic and technical support for the integration and calibration activities.

The VLDA assembly was provided by MPS under Contract 2013-058-I.0 with the Italian Space Agency (ASI). The UVDA assembly was provided by MPS as German contribution to Metis thanks also to the financial support of DLR (grant 50 OT 1201). The primary and secondary mirrors were provided as Czech contribution to Metis; the mirror hardware development was possible thanks to the Czech PRODEX Programme.

The authors would like to thank the Metis team of THALES Alenia Space Italia for their support; in particular: S. Cesare, R. Boccardo, R. Brando, C. Baietto, R. Bertone, and P. Sandri of OHB Italia for the fruitful discussion on the telescope alignment procedure and related obtained results.

REFERENCES

- [1] Muller, D., Marsden, R. G., StCyr, O. C., and Gilbert H. R., "Solar Orbiter: Exploring the Sun-heliosphere connection," *Solar Physics* 285 (1-2), 25-70 (2013).
- [2] Frassetto, F., et al., "Optical performance of the Metis coronagraph on the Solar Orbiter ESA mission," to be published in this Proc. SPIE volume, (2018).
- [3] Mottini, S., "Alignment specification for Metis PFM," METIS-TASI-SPE-025, (2016).
- [4] Fineschi, S., Antonucci, E., Romoli, M., Bemporad, A., Capobianco, G., Crescenzo, G., Nicolini, G., Massone, G., Telloni, D., Focardi, M., Landini, F., Pancrazzi, M., Poletto, L., Pelizzo, M.-G., Da Deppo, V., Moses, J. D., Andretta, V., Naletto, G., Nicolosi, P., Spadaro, D., Berlicki, A., Uslenghi, M., Malvezzi, M., Teriaca, L., Abbo, L., Magli, E., "Novel space coronagraphs: METIS, a flexible optical design for multi-wavelength imaging and

- spectroscopy," Proc. SPIE 8862, 88620G (2013).
- [5] Romoli, M., Landini, F., Antonucci, E., Andretta, V., Berlicki, A., Fineschi, S., Moses, J. D., Naletto, G., Nicolosi, P., Nicolini, G., Spadaro, D., Teriaca, L., Baccani, C., Focardi, M., Pancrazzi, M., Pucci, S., Abbo, L., Bemporad, A., Capobianco, G., Massone, G., Telloni, D., Magli, E., Da Deppo, V., Frassetto, F., Pelizzo, M. G., Poletto, L., Uslenghi, M., Vives, S., Malvezzi, M., "METIS: the visible and UV coronagraph for solar orbiter," Proc. SPIE 10563, 105631M (2017).
- [6] Landini, F., et al., "Stray light calibration for the Solar Orbiter/Metis solar coronagraph," to be published in this Proc. SPIE volume, (2018).
- [7] Sandri, P., et al., "Stray-light analyses of the multielement telescope for imaging and spectroscopy coronagraph Solar orbiter," Opt. Eng. 57(1), 015108 (2018).
- [8] Nardello, M., Zuccon, S., Corso, A. J., Zuppella, P., Gerlin, F., Tessarolo, E. and Pelizzo, M. G., "Study of optical materials to be used on Multi Element Telescope for Imaging and Spectroscopy instrument," Journal of Astronomical Telescopes, Instruments, and Systems 1, 024003 (2015).
- [9] Zuppella, P., Monaco, G., Corso, A. J., Nicolosi, P., Windt, D. L., Bello, V., Mattei, G. and Pelizzo, M. G., "Iridium/silicon multilayers for extreme ultraviolet applications in the 20-35 nm wavelength range," Opt. Lett. 36(7), 1203-1205 (2011).
- [10] Silva-López, M., Bastide, L., Restrepo, R., García Parejo, P. and Álvarez-Herrero, A., "Evaluation of a liquid crystal based polarization modulator for a space mission thermal environment," Sensors and Actuators A: Physical 266, 247-257 (2017).
- [11] Capobianco, G., Casti, M., Fineschi, S., Massone, G., Sertsu, M. G., Landini, F., Romoli, M., Antonucci, E., Andretta, V., Naletto, G., Nicolini, G., Spadaro, D., Alvarez Herrero, A., Garcia Parejo, P. and Marmonti M., "Wide field of view liquid crystals-based modulator for the polarimeter of the Metis/Solar Orbiter," Proc. SPIE 10698, 1069830 (2018).
- [12] Fischer, R. E., Tadic-Galeb, B., and Yoder, P. R., [Optical System Design], McGraw Hill, (2008).
- [13] Da Deppo, V., Crescenzo, G., Naletto, G., Fineschi, S., Romoli, M. and Antonucci, E., "Preliminary tolerance analysis of the coronagraphic instrument METIS for the Solar Orbiter ESA mission," Proc. SPIE 8862, 88620X (2013).
- [14] Da Deppo, V., Poletto, L., Crescenzo, G., Fineschi, S., Antonucci, E. and Naletto, G., "Preliminary error budget analysis of the coronagraphic instrument metis for the solar orbiter ESA mission," Proc. SPIE 10564, International Conference on Space Optics - ICSO 2012, 105643B (2017).